applied sciences

MDPI

Article

Long-Term Behaviour of Precast Concrete Deck Using Longitudinal Prestressed Tendons in Composite I-Girder Bridges

Haiying Ma, Xuefei Shi * and Yin Zhang

Department of Bridge Engineering, Tongji University, Shanghai 200092, China; mahaiying@tongji.edu.cn (H.M.); zhangyinzian@126.com (Y.Z.)

* Correspondence: shixf@tongji.edu.cn; Tel.: +86-216-598-2956

Received: 12 November 2018; Accepted: 5 December 2018; Published: 13 December 2018

Abstract: Twin-I girder bridge systems composite with precast concrete deck have advantages including construction simplification and improved concrete strength compared with traditional multi-I girder bridge systems with cast-in-place concrete deck. But the cracking is still a big issue at interior support for continuous span bridges using twin-I girders. To reduce cracks occurrence in the hogging regions subject to negative moments and to guarantee the durability of bridges, the most essential way is to reduce the tensile stress of concrete deck within the hogging regions. In this paper, the prestressed tendons are arranged to prestress the precast concrete deck before it is connected with the steel girders. In this way, the initial compressive stress induced by the prestressed tendons in the concrete deck within the hogging region is much higher than that in regular concrete deck without prestressed tendons. A finite element analysis is developed to study the long-term behaviour of prestressed concrete deck for a twin-I girder bridge. The results show that the prestressed tendons induce large compressive stresses in the concrete deck but the compressive stresses are reduced due to concrete creep. The final compressive stresses in the concrete deck are about half of the initial compressive stresses. Additionally, parametric study is conducted to find the effect to the long-term behaviour of concrete deck including girder depth, deck size, prestressing stress and additional imposed load. The results show that the prestressing compressive stress in precast concrete deck is transferred to steel girders due to concrete creep. The prestressed forces transfer between the concrete deck and steel girder cause the loss of compressive stresses in precast concrete deck. The prestressed tendons can introduce some compressive stress in the concrete deck to overcome the tensile stress induced by the live load but the force transfer due to concrete creep needs be considered. The concrete creep makes the compressive stress loss and the force redistribution in the hogging regions, which should be considered in the design the twin-I girder bridge composite with prestressed precast concrete deck.

Keywords: concrete creep; prestressing stress; compressive stress; FE analysis; force transfer

1. Introduction

A two or multiple-I girder system has two or more steel I girders connected with diaphragms and composite with a concrete deck using shear studs. The steel girders are in tension and the concrete deck is in compression in the regions of positive moments (i.e., the sagging region) under vertical loads, which makes good use of material advantages of steel and concrete. While within the regions of negative moments (i.e., the hogging regions), the concrete deck is in tension under vertical loads and the tensile stress may increase due to concrete shrinkage and creep. Concrete cracking is a big issue for the hogging regions [1–5]. High performance concrete with larger tension strength can be

used [6] but the cost is substantial. One common way to make concrete deck in compression with initial compressive stress to overcome the tensile stress induced by live load.

One way is to arrange prestressed tendons in the concrete deck in the hogging regions. The prestressing compressive stress in the concrete is to overcome any additional tensile stress induced by vertical loads and additional second order effect of shrinkage and creep. Miyamoto et al. found that using external tendons could be considered an effective method of strengthening bridges deteriorating due to overloading [7]. Deng and Morcous proposed a new prestressed concrete-steel composite girder, which uses pretensioned concrete bottom flange to provide initial compressive stress in the concrete deck [8,9]. Wang et al. investigated the behaviour of reinforced concrete strengthened with externally prestressed tendons and they found that the basalt fibre reinforced polymer (BFRP) was feasible to strengthen the beam behaviour [10].

Except using tendons to introduce compressive stress in concrete deck, some construction strategies are used. Temporary loads are sometimes applied to the sagging regions (the regions of positive moment) before the concrete cast in the hogging regions. In this way, the compressive stress is induced in the hogging regions after the hogging region concrete is hardened and the temporary loads are removed. Marí et al. and Dezi et al. studied the behaviour of composite bridges considering different construction processes and they found that the construction sequence could affect the tension stress in concrete deck in the hogging regions [11,12]. Liu et al. analysed the jacking-up method to prestress the concrete deck and they found that jacking-up the interior support could efficiently introduce compressive stress in the concrete deck in the hogging regions to overcome the tensile stresses induced by shrinkage and live load [13].

Either prestressed tendons or construction strategies can introduce initial compressive stress in the concrete deck to avoid or reduce concrete cracking in the hogging regions. However, for the preconnected composite girder systems, the prestressed forces are applied to the whole composite section and mostly are applied to the steel section. Kwon et al. and Hällmark et al. studied the behaviour of steel-concrete composite girders with prestressing tendons before concrete deck connected to steel girders [14,15]. Su et al. studied the behaviour of a continuous composite box girder with prefabricated prestressed concrete slab in the hogging region [16]. Tong et al. studied the long-term behaviour of the composite box girders with post connected prestressed concrete deck and the research shows the prestressed concrete deck before connected with steel box girders can improve concrete shrinkage [17].

In recent years, a significant amount of continuous twin-I girders with precast concrete deck are built in China. The cracks in the hogging regions are usually controlled by the crack width control [18–20]. However, crack width control is not an efficient way to improve the behaviour in the hogging regions. The way to arrange prestressed tendons in concrete deck in the hogging regions is used for twin-I girders with post connected prestressed precast concrete deck. In the paper, the long-term behaviour of a continuous twin-I girder bridge is investigated to find the creep effect on the compressive stresses induced by the prestressed tendons. Additionally, parametric study is developed to find the creep effect on the prestressing the concrete deck and the force transfer between steel girders and concrete deck.

2. Case of a Twin-I Girder Composite with Precast Deck

The bridge is composed of steel two-I girders with precast concrete deck and the steel girders and precast concrete deck are composite with shear studs within the voids. The span arrangement is 4×35 m. The girder spacing is 8.95 m. The steel girder depth is 1.7 m. Cross beams are arranged with a spacing of 7 m. Interior cross beams are not connected with the concrete deck and end cross beams at the ends of bridge are connected with the concrete deck through the shear studs. The width of the precast concrete deck is 16.75 m. For the concrete deck, the prestressed tendons are arranged in the hogging regions. Figure 1 presents the structure components in the hogging regions of the bridge.

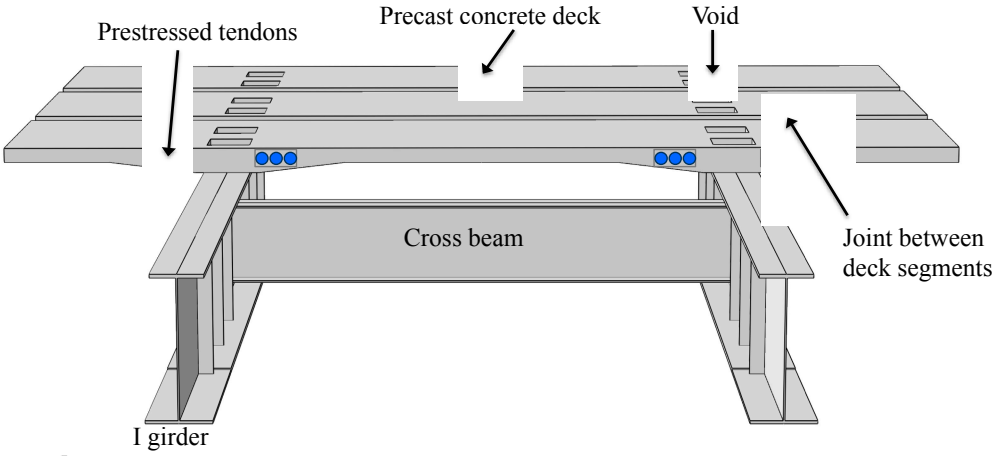

Figure 1. A continuous twin-I girder with prestressed precast concrete deck in the hogging region.

As shown in Figure 2, the construction procedure including five steps:

(1) The steel girders are lifted and connected to be a four-span continuous system.
(2) All the precast concrete segments are lifted to the steel girders and the concrete deck and the steel girders are not composite (the concrete in the voids are not casted).
(3) Only the precast concrete deck segments within the hogging regions (e.g., within the regions at interior supports) are prestressed and the steel girders are not composite with the concrete deck at this time.
(4) The joints and voids are casted with concrete to make the concrete deck composite with the steel girders.
(5) The transverse tendons are prestressed and the bridge is constructed with the wearing surface and the attached appurtenances (barriers, railings, lights, etc.).

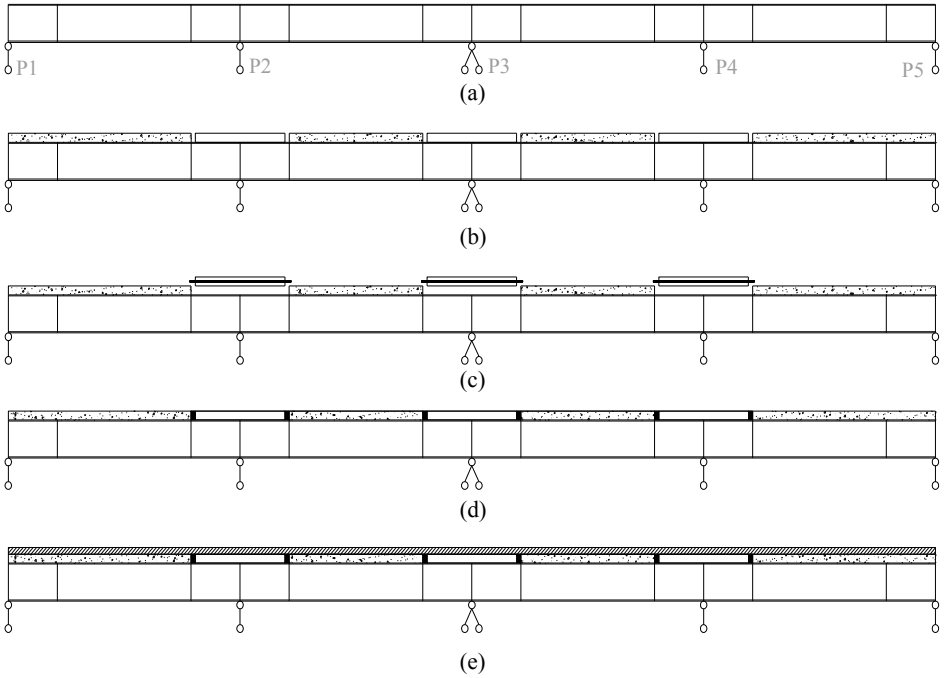

Figure 2. Construction sequence of the twin-I girder bridge: (**a**) Steel girder erection; (**b**) Precast concrete deck segments erection; (**c**) Prestressing concrete deck in the hogging regions; (**d**) Cast-in-place joints and void to connect girders and deck; (**e**) Constructed condition with the wearing surface and the attached appurtenance.

3. Finite Element Model

3.1. Elements and Meshes

The software ANSYS is used to develop analysis in the paper [21,22]. FE analyses can predict and analyse the behaviour of steel-composite bridges [1,9,16,23]. Solid elements (element type of solid 45) are used to model a concrete deck and shell elements (element type of shell 43) are used to model steel girders and stiffeners. Spring element (element type of combine14) is used to model shear studs to connect the concrete deck and steel girders. The concrete deck and the steel girders are assumed fully connected by the shear studs. Link elements (element type of link 8) are used to model prestressed tendons. The prestress forces in the tendons are applied with temperature. Figure 3 shows the finite element model of the bridge. The default convergence criteria are used in the analyses.

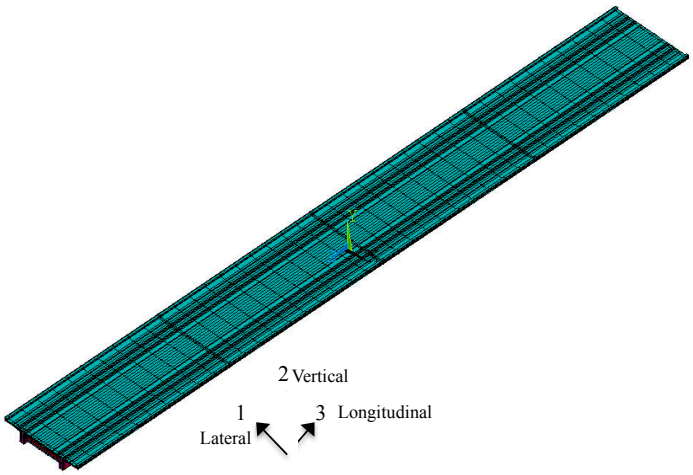

Figure 3. Finite element model of a twin-I girder bridge with precast concrete deck.

3.2. Material Models

The steel material of the girders is modelled using an elastic isotropic material in the elastic range with an elastic modulus of 200 GPa and Poisson's ratio of 0.3 and a perfectly plastic isotropic material in the inelastic range. The yield strength of the steel material is 345 MPa. The deck concrete has 23.1 MPa compressive strength (Ministry of Transport of the People's Republic of China) [19,22,23]. An empirical stress-strain model for unconfined concrete proposed by Oh and Sause is used for the uniaxial stress-strain relationship of concrete [24].

The creep and shrinkage are included in the model based on the equations from Ministry of Transport of the People's Republic of China [25]. The shrinkage effect is applied to the models through temperature decrease in the concrete material. ANSYS does not have direct method to calculate the creep effect. It gives metal creep model to model the creep in concrete. There are 13 creep equations in ANSYS and one used often is as follows:

$$\dot{\varepsilon_{cr}} = C_1 \sigma^{C_2} \varepsilon_{cr}^{C_3} e^{-C4/T} \quad (1)$$

where, ε_{cr} is creep strain; $\dot{\varepsilon_{cr}}$ is creep variance ratio of time; σ is stress; T is absolute temperature; C1 through C4 is parameters to be calculated. Usually, there are two ways to simplify the equation. One is to assume that creep variance ratio of time is only related to stress with C2 = 1 and C3 = C4 = 0 (Method A). Thus the equations is simplified as follows:

$$\Delta\varepsilon_{cr} = C_1 \sigma \Delta t \quad (2)$$

For concrete with constant stress, the creep strains satisfy:

$$\varepsilon_{cr} = \varepsilon_0 \phi(t, t_0) = \frac{\sigma_0}{E} \phi(t, t_0) \tag{3}$$

Equation (3) is changed with time of Δt:

$$\frac{\Delta \varepsilon_{cr}}{\Delta t} = \varepsilon_0 \phi(t, t_0) = \frac{\sigma_0}{E} \frac{\Delta \phi(t, t_0)}{\Delta t} \tag{4}$$

Within the time of Δt, C1 is calculated as follows:

$$C_i = \frac{\Delta \phi(t_i, t_{i-1})}{\Delta t} \frac{1}{E} \tag{5}$$

Another way is assuming there is linear relationship between creep variation rate and strain with C2 = C4 = 0, C3 = 1 (Method B), which is denoted as follows:

$$\Delta \varepsilon_{cr} = C_1 \varepsilon \Delta t \tag{6}$$

For concrete with constant stress, the creep strains satisfy:

$$\varepsilon(t) = \varepsilon_e + \varepsilon_c(t) = (1 + \phi(t, t_0))\varepsilon_e \tag{7}$$

Thus within the time of Δt, C1 is calculated as follows:

$$C1 = \frac{\Delta \phi(t_i, t_{i-1})}{\Delta t(1 + \phi(t_i, t_{i-1}))} \tag{8}$$

Figure 4 presents the validation of these two ways to analyse the creep effect for a column applied with a vertical constant force (denoted as *P*) and shows that the ways agree with the results using theoretical analysis.

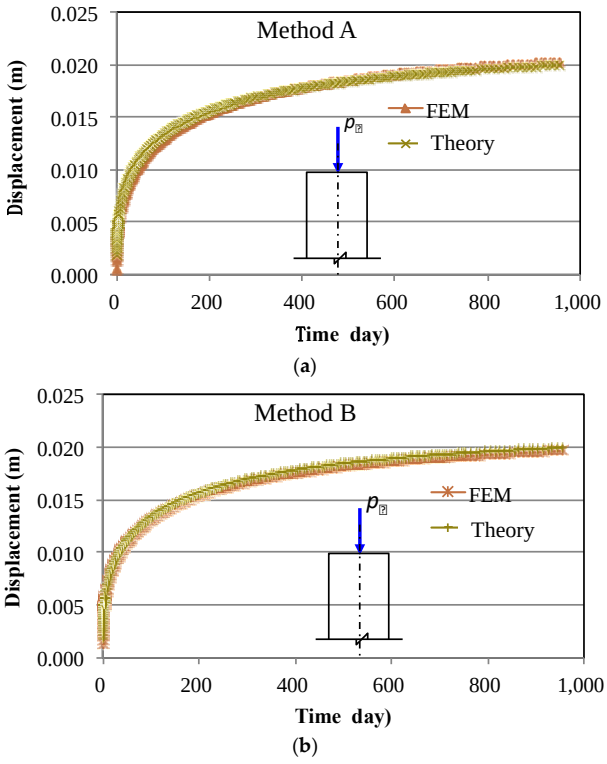

Figure 4. Finite element analysis using metal creep model for creep effect: (**a**) Method A; (**b**) Method B.

3.3. Boundary Conditions

Continuously supported boundary conditions are used for the bridge model. The vertical displacements (*U2*) at the bottom of the flange nodes are restrained at each support. At each support, the lateral displacements (*U1*) of the bottom flange nodes at the bottom of the flange nodes are restrained. The longitudinal displacements (*U3*) of the bottom flange nodes at the middle support are only restrained.

4. Long-Term Behaviour Analysis

4.1. Prestressed Concrete Deck Condition

Table 1 gives the induced compressive stresses in the precast concrete deck within the hogging regions. After the tendons prestressed, the compressive stresses on the deck top surface are from −6 Mpa to −7 Mpa (negative value denotes compression) and are from −7 Mpa to −8 Mpa on the deck bottom surface. The tendons are not located at the neutral axis of the deck cross-section and cause the difference between the top surface and the bottom surface.

Table 1. Stress and deformation analysis results.

Analysis Result		Prestressed Concrete Deck Condition	Constructed Condition	10,000-Day Creep
Concrete deck	Bottom surface	−7~−8 MPa	−4.4~−6.2 MPa	−2.3 MPa~−3.3 MPa
	Top surface	−6~−7 MPa	−4.7~−5.6 MPa	−2.6 MPa~−3.5 MPa
Steel girder	Top flange	135 Mpa	165 MPa	10–20 MPa
	Bottom flange	143 MPa	167 MPa	155–165 MPa
Tendons		-	1135–1175 MPa	1115–1180 MPa
Deflection		0.066 m	0.074 m	0.040 m

4.2. Constructed Condition

Figures 5 and 6 present the normal stress variation in the concrete deck and the steel girders under the bridge constructed condition. Within the hogging regions, the compressive stresses vary from −5.6 MPa to −6.4 MPa at middle interior support (P3) and vary from −4.7~−5.6 MPa at the other interior supports (P2 and P4). The maximum tension stresses in the steel girders are about 165 MPa at P2. After the bridge constructed, the compressive stresses in the concrete deck within the hogging regions are not small.

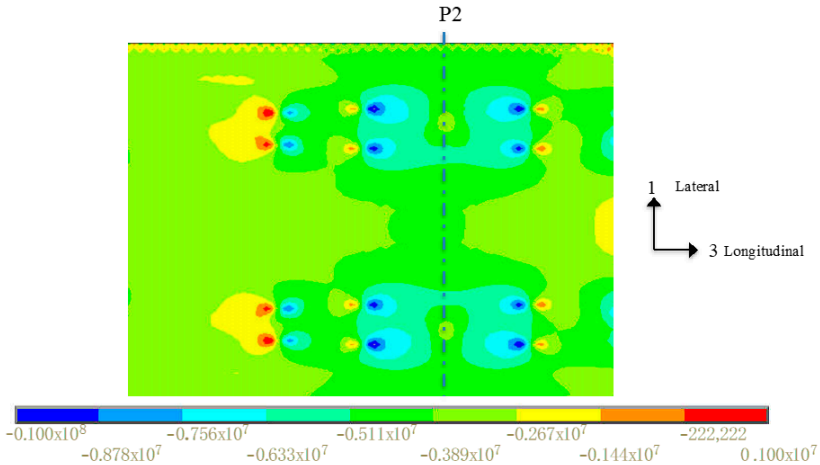

Figure 5. Stress at the top surface of the concrete deck under the constructed condition in the hogging region (Pa).

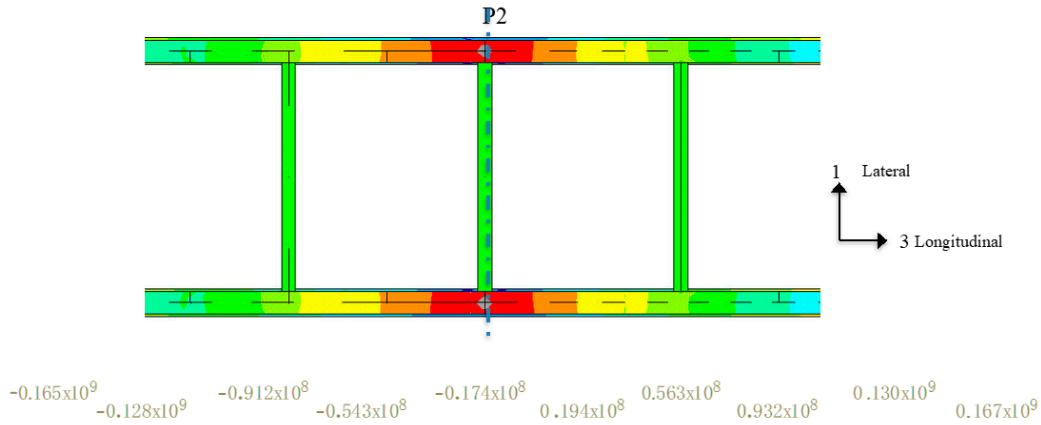

Figure 6. Stress at the top flange of the steel girders under the constructed condition in the hogging region (Pa).

4.3. Long-Term Behaviour

Figure 7 shows the normal stress variation on the concrete deck top surface after 10,000 days creep near P2. Compared with the stresses under the constructed condition, the stresses in the concrete deck change due to the concrete creep, especially in the hogging regions. The compressive stresses decrease to −2.6~−3.5 MPa, with a decrease of about 3 MPa from the constructed condition. Figure 8 presents the stress variation in the steel girder. The flange stresses in the girder change a lot compared with the constructed condition that top flange stress is in compression with stress from −10 to −20 MPa. The stresses in the tendons are checked and it is found that no changes occur for the tendons. The results show that the concrete creep reduces the initial compressive stress in the concrete deck and causes force transfer between the concrete deck and the steel girders.

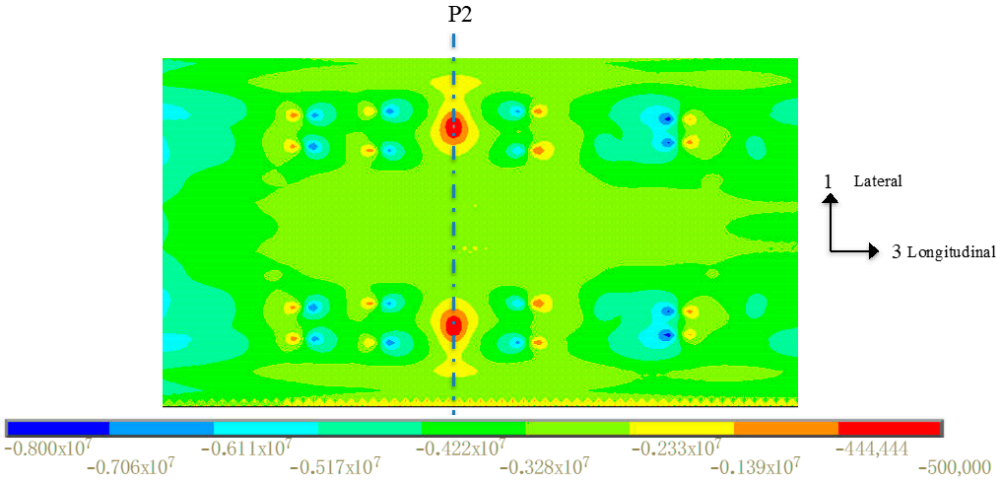

Figure 7. Stress at the top surface of the concrete deck in the hogging region after 10,000-day creep (Pa).

Table 1 summarizes the stress change in the bridge due to the concrete creep. The results show that the stresses in the concrete deck and the steel girders change due to the concrete creep. The force transfer occurs between the concrete deck and the steel girders and it mostly occurs within the hogging regions.

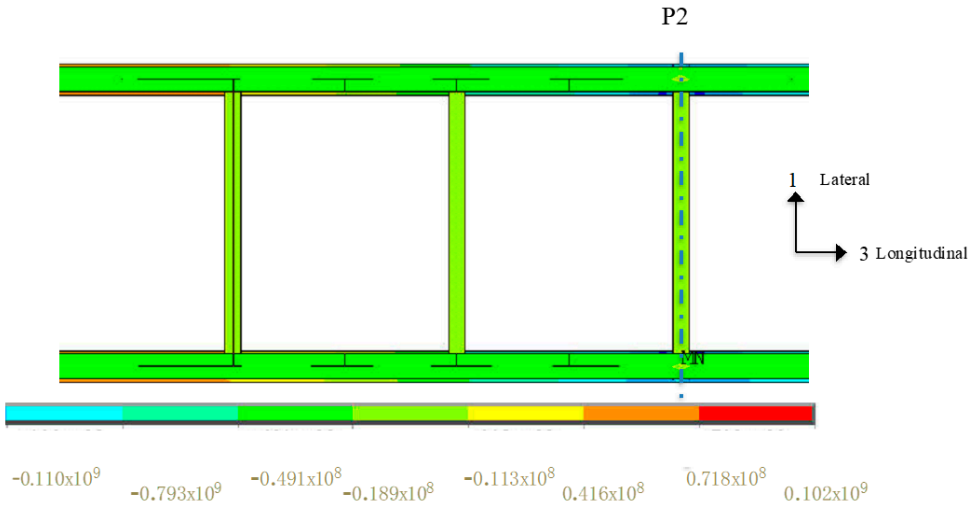

Figure 8. Stress at the top flange of the steel girders in the hogging region after 10000-day creep (Pa).

5. Parametric Studies

To study the effects of different parameters on the prestressing the concrete deck and the force transfer between the concrete deck and steel girders, a simplified two-span I girder is conducted. The continuous girder has two spans of 3 m + 3 m. The precast concrete deck has width of 0.5 m. The parameters include girder depth, concrete deck thickness, prestressed compressive stress in concrete deck and additional imposed vertical load. The additional imposed load is to model the condition that long-term load applied on the bridge system. Note that 10,000 days creep is considered in the analyses.

5.1. Girder Depth

Different girder depths are analysed and discussed to find the effect of girder stiffness on the creep effect. Figure 9 gives the stress variation in the hogging region. The initial prestressing stress is 10 MPa. Along with the increase of girder depth, the stress variations due to shrinkage and creep decrease slightly, which indicates that the girder stiffness has little effect on the creep effect. The results also show that the stress loss due to creep is over than 50% of the initial prestressing stress. The stresses in the tendons do not change and the stress loss in the concrete deck is transferred to steel girders.

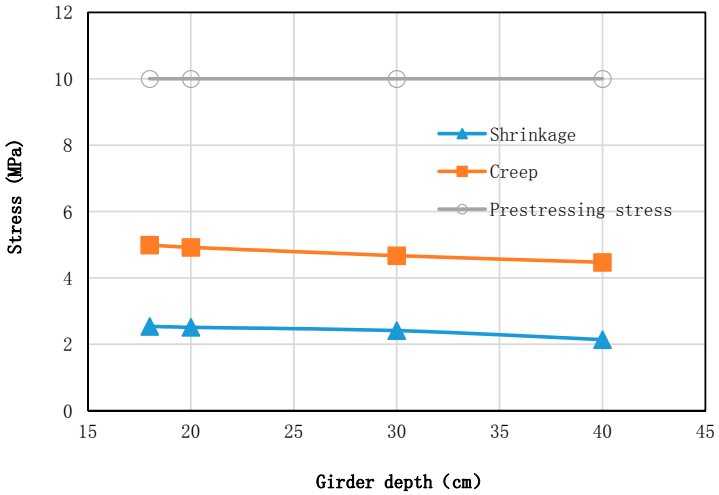

Figure 9. Stress variation in the concrete deck in the hogging region due to different effects for different girder depths.

5.2. Deck Thickness

Different deck thickness are analysed and discussed to find the effect of deck size on the creep effect. Figure 10 presents the stress variation in the hogging region. The initial prestressing stress is 10 MPa. The results show that the stresses due to shrinkage have no change with the increase of deck thickness. Along with the increase of deck thickness, the stress variations due to creep varies but the variation is not linear. The stress variation induced by creep increases with the increase the deck thickness up to 180 mm thickness and then decreases. With the thickness of 180 mm, the stress loss is the biggest one. But the difference is not big and the difference between the thickness of 180 mm and 160 mm is 6%. The results also show that the stress loss due to creep is over than 50% of the initial prestressing stress.

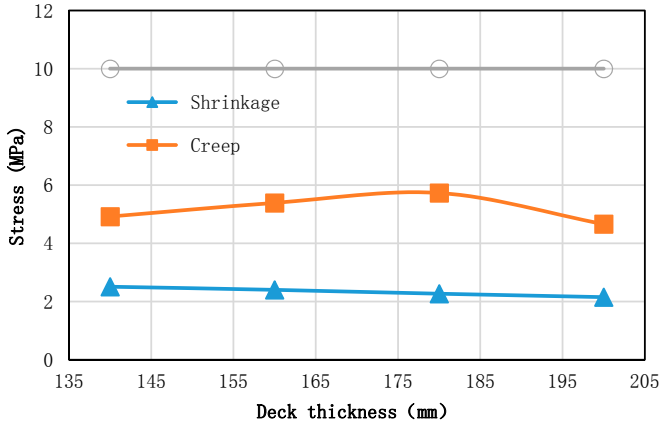

Figure 10. Stress variation in the concrete deck in the hogging region due to different effects for different deck thicknesses.

5.3. Prestressing Stress

Figure 11 presents the results to analyse the initial prestressing stress applied to concrete deck. The stress due to shrinkage has no change with the increase of prestressing stress. Along with the increase of the initial prestressing stress, the stress loss due to creep increases. The ratio between the stress loss due to creep to the initial prestressing stress is larger for smaller prestressing stress (e.g., 67% for 5 MPa prestressing stress and 49% for 10 MPa prestressing stress). The results show that the prestressing stress is decreased in the concrete deck due to creep and the loss mostly is larger than 50% of the initial prestressing stress.

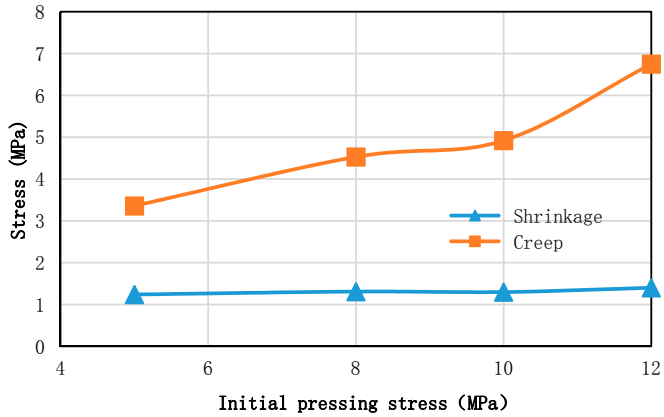

Figure 11. Stress variation in the concrete deck in the hogging region due to different effects for different prestressing stress by tendons.

5.4. Additional Imposed Load

Additional imposed load is to model the condition under long-term dead load and live load, which induces tension in the concrete deck in the hogging regions. The tension stress induced by the additional imposed load is used to denote the value of the imposed load. Figure 12 presents the results to analyse the effect of additional imposed load to the creep effect. In the figure, "shrinkage" denotes the stress variation induced by the concrete shrinkage, "creep" denotes the stress variation induced by the concrete creep considering 10,000 days and "prestressing stress" denotes the initial compressive stress introduced by the prestressed tendons. The initial prestressing stress is 10 MPa. The stress due to shrinkage has no change with the increase of additional imposed load. With the increase of imposed load, the stress loss due to creep increase, which shows that the additional imposed load have a big effect on the creep effect.

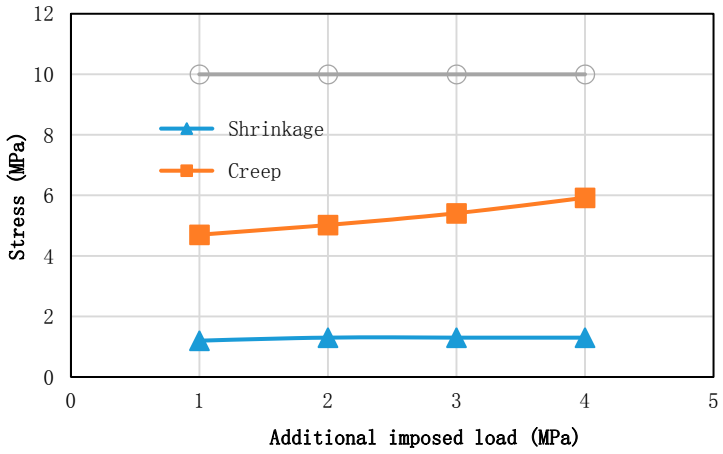

Figure 12. Stress variation in the concrete deck in the hogging region due to different effects for different additional imposed load.

6. Conclusions

The paper investigated the behaviour of a four-span continuous twin-I girder bridge using prestressed precast concrete deck due to concrete creep. Simplified two-span I girder models are analysed to find the effect on the prestressed compression and force transfer between concrete deck and steel girders. Major findings are summarized as follows:

(1) For the continuous twin-I girder bridge, the prestressed tendons introduce compressive stress in the concrete deck and the compressive stress under constructed condition is big and it can overcome the tensile stress induced by shrinkage and live load.

(2) In the hogging regions, the prestressed stresses in the concrete deck are reduced due to the concrete creep effect and the decrease is up to 50% of the initial prestressing stress.

(3) The stresses in the steel girders in the hogging regions vary big, especially for girder flange in tension and the changes are due to force transfer from compressive stress in concrete deck.

(4) The stresses in the tendons have almost no change and the prestressed force transfers from concrete deck to steel girders in the hogging regions.

(5) The steel girder stiffness has no effect on the prestressing stress loss in the concrete deck.

(6) The concrete deck, initial prestressing stress and additional imposed load have an effect on the initial prestressing stress loss in the concrete deck due to concrete creep.

(7) The prestressing stress loss in the concrete due to creep mostly is over 50% and it is transferred to steel girders to change the stress distribution of composite section in the hogging regions.

Author Contributions: Conceptualization, H.M. and X.S.; numerical analysis, H.M., X.S. and Y.Z.; writing: H.M. and Y.Z.

Funding: This research was funded by National Key R&D Program of China, grant number 2018YFC0809606, National Natural Science Foundation of China, grant number 51608378 and Science and Technology Commission of Shanghai Municipality (18DZ1201203, 17DZ1204300) and the Fundamental Research Funds for the Central Universities.

Conflicts of Interest: The authors declare no conflict of interest.

References

1. Gara, F.; Leoni, G.; Dezi, L. Slab cracking control in continuous steel-concrete bridge decks. *J. Bridge Eng.* **2013**, 1319–1327. [CrossRef]
2. Macorini, L.; Fragiacomo, M.; Amadio, C.; Izzuddin, B.A. Long-term analysis of steel–concrete composite beams: FE modeling for effective width evaluation. *Eng. Struct.* **2006**, *28*, 1110–1121. [CrossRef]
3. Oehlers, D.J.; Bradford, M.A. *Composite Steel and Concrete Structures: Fundamental Behavior*; Elsevier: Oxford, UK, 2013.
4. Ryu, H.K.; Chang, S.P.; Kim, Y.J.; Kim, B.S. Crack control of a steel and concrete composite plate girder with prefabricated slabs under hogging moments. *Eng. Struct.* **2005**, *27*, 1613–1624. [CrossRef]
5. Xia, Y.; Wang, P.; Sun, L. Neutral axis position based health monitoring and condition assessment techniques for concrete box girder bridges. *Int. J. Struct. Stab. Dyn.* **2019**, *19*. [CrossRef]
6. Xia, Y.; Nassif, H.; Su, D. Early-age cracking in high performance concrete decks of typical Curved steel girder bridges. *J. Aerosp. Eng. (ASCE)* **2017**, *30*, B4016003. [CrossRef]
7. Miyamoto, A.; Tei, K.; Nakamura, H.; Bull, J. Behavior of prestressed beam strengthened with external tendons. *J. Struct. Eng.* **2000**, 1033–1044. [CrossRef]
8. Deng, Y.; Morcous, G. Efficient prestressed concrete-steel composite girder for medium-span bridges. I: System description and design. *J. Bridge Eng.* **2013**, 1347–1357. [CrossRef]
9. Deng, Y.; Morcous, G. Efficient prestressed concrete-steel composite girder for medium-span bridges. II: Finite-element analysis and experimental investigation. *J. Bridge Eng.* **2013**, 1358–1372. [CrossRef]
10. Wang, X.; Shi, J.; Wu, G.; Yang, L.; Wu, Z. Effectiveness of basalt FRP tendons for strengthening of RC beams through the external prestressing technique. *Eng. Struct.* **2015**, *101*, 34–44. [CrossRef]
11. Marí, A.; Mirambell, E.; Estrada, I. Effects of construction process and slab prestressing on the serviceability behaviour of composite bridges. *J. Constr. Steel Res.* **2003**, *59*, 135–163. [CrossRef]
12. Dezi, L.; Gara, F.; Leoni, G. Construction sequence modeling of continuous steel-concrete composite bridge decks. *Steel Compos. Struct.* **2006**, *6*, 123–138. [CrossRef]
13. Liu, X.; Liu, Y.; Luo, J.X.H. Behavior of Continuous Composite Bridge during Construction with Jacking up Interior Support, National Bridge Conference 2012, pp. 658–662, 2012. (In Chinese). China Highway and Transportation Society. Available online: http://caj.d.cnki.net//KDoc/docdown/pubdownload.aspx?dk=kdoc%3apdfdown%3aa31df52a5345b1bdc7ff1d792e853f28 (accessed on 12 November 2018).
14. Kwon, G.; Engelhardt, M.D.; Klingner, R.E. Behavior of post-installed shear connectors under static and fatigue loading. *J. Constr. Steel Res.* **2010**, *66*, 532–541. [CrossRef]
15. Hällmark, R.; Collin, P.; Möller, M. The behaviour of a prefabricated composite bridge with dry deck joints. *Struct. Eng. Int.* **2013**, *23*, 47–54. [CrossRef]
16. Su, Q.; Yang, G.; Bradford, M. Behavior of a continuous composite box girder with a prefabricated prestressed-concrete slab in its hogging-moment region. *J. Bridge Eng.* **2015**, B4014004. [CrossRef]
17. Tong, T.; Yu, X.; Su, Q. Coupled effects of concrete shrinkage, creep, and cracking on the performance of postconnected prestressed steel-concrete composite girders. *J. Bridge Eng.* **2017**. [CrossRef]
18. Ministry of Construction of the People's Republic of China. *Code for Design of Concrete Structures*; GB50010-2010; Ministry of Construction of the People's Republic of China: Beijing, China, 2015.
19. Ministry of Transport of the People's Republic of China. *Chinese Code for Design of Highway Reinforced Concrete and Pre-Stressed Concrete Bridge and Culverts Beijing*; JTG D62-2004; Ministry of Transport of the People's Republic of China: Beijing, China, 2004.
20. Ministry of Transport of the People's Republic of China. *Code for Design of Highway Reinforced Concrete and Prestressed Concrete Bridges and Culverts*; JTG D62-2012; Ministry of Transport of the People's Republic of China: Beijing, China, 2012.
21. *ANSYS Release 12.0 [Computer Software, version 12.0]*; ANSYS, Inc.: Canonsburg, PA, USA, 2009.

22. ANSYS, Inc. *ANSYS Manual*; ANSYS, Inc.: Canonsburg, PA, USA, 2009.
23. Pan, H.; Azimi, M.; Yan, F. Time-Frequency-Based Data-Driven Structural Diagnosis and Damage Detection for Cable-Stayed Bridges. *J. Bridge Eng.* **2018**, *23*, 04018033. [CrossRef]
24. Ministry of Construction of the People's Republic of China. *Code for Design of Steel Structures*; GB50017-2003; Ministry of Construction of the People's Republic of China: Beijing, China, 2003.
25. Ministry of Construction of the People's Republic of China. *Code for Design of Steel and Concrete Composite Bridges*; GB50917-2013; Ministry of Construction of the People's Republic of China: Beijing, China, 2013.
26. Oh, B.; Sause, R. Empirical Models for Confined Concrete under Uniaxial Loading. In *International Symposium on Confined Concrete*; ACI SP-238; American Concrete Institute: Farmington Hills, MI, USA, 2006; pp. 141–156.